

# Ice shelf thickness over Larsen C, Antarctica, derived from satellite altimetry

J. A. Griggs<sup>1</sup> and J. L. Bamber<sup>1</sup>

Received 8 June 2009; revised 24 July 2009; accepted 2 September 2009; published 3 October 2009.

[1] Satellite radar altimetry can be used to infer the thickness of floating ice shelves around Antarctica under the assumption of hydrostatic equilibrium. Ice shelf thickness is an essential parameter in mass budget calculations and is one of the more poorly characterised. Using data from the ERS-1 radar altimeter recorded in 1994–5, we calculate the thickness of Larsen C ice shelf on the Antarctic Peninsula. The surface elevation was determined to an accuracy of  $-2.3 \pm 4.35$  m as compared to elevations from the laser altimeter onboard ICESat. Using a model for firm depth and density, we created a 1 km grid of ice shelf thickness for Larsen C. The accuracy of the ice thickness retrieval was determined from independent airborne radio echo sounding data. The results indicated a bias of  $-0.22$  m and random error of 36.7 m, which is equivalent to 12.7% of the mean thickness for this ice shelf. **Citation:** Griggs, J. A., and J. L. Bamber (2009), Ice shelf thickness over Larsen C, Antarctica, derived from satellite altimetry, *Geophys. Res. Lett.*, 36, L19501, doi:10.1029/2009GL039527.

## 1. Introduction

[2] Ice shelf thickness is an important boundary condition for ice sheet and sub shelf cavity ocean modelling and is needed to improve mapping of all the ice shelves in Antarctica. It is also required near the grounding line to calculate the ice fluxes required to determine ice sheet mass balance [Rignot *et al.*, 2008]. In this approach, the accuracy of the ice thickness is one of the constraining parameters on the uncertainty in the estimate [Rignot and Thomas, 2002]. Ice thickness is also required to calculate the sub-shelf mass balance and bottom melting rates based on the principles of conservation of mass.

[3] A number of ice shelves on the Antarctic Peninsula have collapsed in recent decades with large effects on the ice dynamics of the inland grounded glaciers [De Angelis and Skvarca, 2003; Rignot *et al.*, 2004a; Rott *et al.*, 1996; Scambos *et al.*, 2004]. There is now considerable interest in whether Larsen C, the largest remaining ice shelf on the Peninsula, will suffer the same fate. Accurate estimates of ice shelf thickness are important for modelling this potential disintegration.

[4] Ice thicknesses can be determined from in situ radio echo sounding measurements but these data provide, in general, rather sparse spatial coverage and a snapshot in time [Fricker *et al.*, 2001; Holland *et al.*, 2009]. Ice thickness can also be estimated from the surface elevation

of floating ice if it is in hydrostatic equilibrium [Bamber and Bentley, 1994]. Satellite altimetry has dramatically increased the accuracy and coverage of elevation data and the capability to infer the ice thickness of all Antarctic ice shelves now exists.

[5] We present a satellite retrieval of the ice thickness of Larsen C as well as an independent validation and a discussion of the error inherent in the method. Larsen C is the most northerly Antarctic ice shelf and represents, therefore, one of the most challenging to tackle for two reasons: it suffers surface melt, unlike its more southerly neighbors and the data coverage worsens moving northward from the latitudinal limit of the satellite.

## 2. Data

[6] In April 1994, the ERS-1 satellite was placed into a single 336 day cycle. This provides 8.3 km across-track spacing at the Equator reducing to 2 km at 70°S. Comparison of the ERS-1 radar altimeter (RA) data with more recent ICESat laser altimetry shows a bias between the two, however, it is slope dependant and small over the ice shelves [Bamber and Gomez-Dans, 2005]. ERS-1 RA penetration into the ice over Larsen C can not be detected [Shepherd *et al.*, 2003].

[7] The ERS-1 RA is used in preference to the newer ICESat data as the spatial coverage of ICESat is poor at the latitude of Larsen C, with across-track spacing of around 22 km. The ERS-1 RA data are the same as those used as the source for a widely used 5 km DEM of Antarctica [Bamber and Bindshadler, 1997] with the addition of corrections for tidal motion of the ice shelves [Bamber *et al.*, 2009]. Thus the time stamp for the ice thickness estimates is January 1995.

## 3. Methodology

[8] If ice is assumed to be in hydrostatic equilibrium, ice thickness can be calculated as

$$\begin{aligned} H_i &= \frac{(e - \delta)\rho_w}{\rho_w - \rho_i} \\ Z - \delta &= \frac{(e - \delta)\rho_w}{\rho_w - \rho_i} \end{aligned} \quad (1)$$

where  $H_i$  is the equivalent ice thickness, i.e., the thickness if all the ice column was at the density of meteoric ice,  $Z$  is the actual ice thickness,  $e$  is the elevation above mean sea level,  $\delta$  is the firm density correction, i.e., the difference between the actual depth of the firm layer and the depth that the firm would be if it was all at the density of meteoric ice,  $\rho_w$  is the density of water and  $\rho_i$  is the density of meteoric ice.

<sup>1</sup>Bristol Glaciology Centre, School of Geographical Sciences, University of Bristol, Bristol, UK.

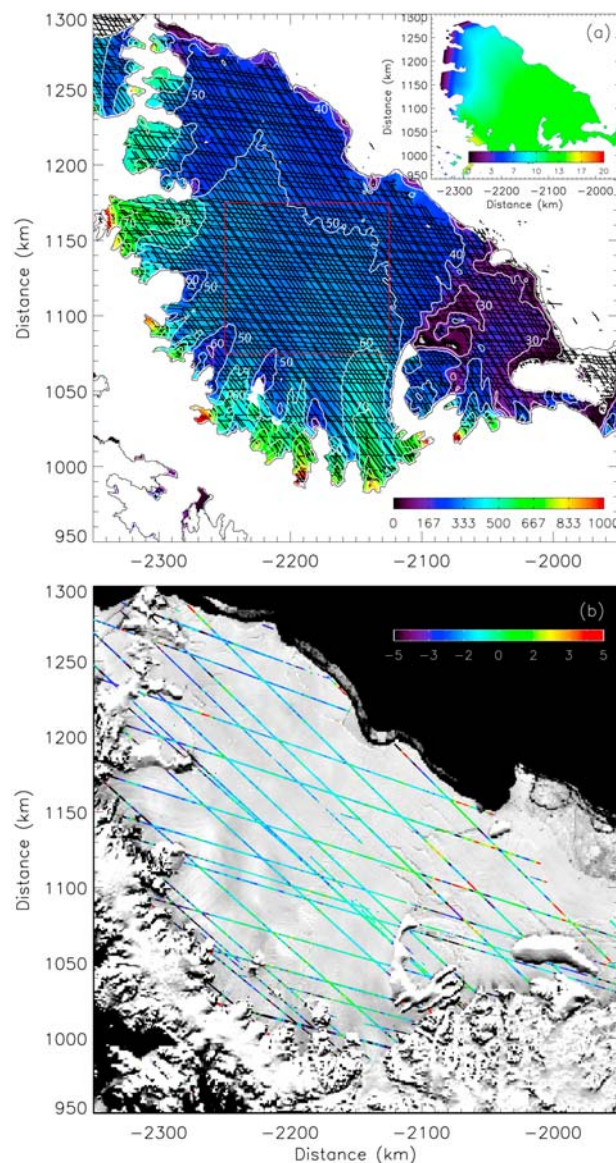


**Figure 1.** (a) ERS-derived ice shelf thickness shown as colored background. Elevation of ERS-1 RA data in metres shown as white contours, and coverage of the data shown as black dots. Axes show distance from the pole in kilometres. Thin black lines are MOA grounding and coast lines, and red box shows the region defined as central area in text. Inset shows the size of the firm density correction. (b) Difference between ERS-derived surface elevation grid and the elevations from ICESat/GLAS overlaid on MOA image of the region.

[9] Hydrostatic equilibrium can only be considered valid when ice is floating freely, which is typically several ice thicknesses from the grounding line. It has been estimated that the elevation profile close to the grounding line passes through the point of hydrostatic equilibrium at the outer boundary of the first fringe of tidal displacement from double-difference Interferometric Synthetic Aperture Radar [Rignot, 1996]. The width of the zone between the grounding line and the point of hydrostatic equilibrium depends on factors including ice rheology and dynamics. Estimates vary

from  $\sim 4.2$  km and 6.4 km for two locations on Institute Ice Stream [Fricker and Padman, 2006] and 9 km on Thwaites Glacier [Rignot, 2001]. Here the grounding line is defined using MODIS mosaic of Antarctica (MOA) [Haran *et al.*, 2005, updated 2006; Scambos *et al.*, 2007] which determines the grounding line from break-in surface slope. This is likely at the grounded side of this zone and so in the  $\sim 10$  km closest to the grounding line, hydrostatic equilibrium may not be valid.

[10] ERS-1 RA data have been corrected for slope-induced error and datapoints were removed where radar lock was lost which can be a particular problem in the grounding zone. Figure 1a shows the available data after geophysical and engineering quality filters were applied. Coverage is almost complete apart from close to the ice front. Data were determined to be over ice using a threshold of 5 m elevation with respect to the geoid [Forste *et al.*, 2008] and floating using the MOA grounding line and grounded islands [Haran *et al.*, 2005, updated 2006; Scambos *et al.*, 2007]. Data were corrected for tidal signatures using the TPX06.2 global tide model [Egbert and Erofeeva, 2002] chosen due to its superior accuracy around Antarctica [King and Padman, 2005].

[11] The elevations were interpolated onto a regular grid using ordinary kriging performed with GSLIB software [Deutsch and Journel, 1997]. A grid spacing of 1 km on a polar stereographic grid of standard parallel  $71^\circ\text{S}$ , central meridian  $0^\circ$  was used resulting in 53% of grid cells containing data. The kriging variogram was modelled as an exponential fit to a variogram calculated from all ERS-1 RA datapoints. A nugget of 1 m was applied and a search radius of 50 km used. The kriging routine averages between 3 and 50 datapoints per grid cell. The results of this interpolation are shown as the white contours in Figure 1a.

[12] The EIGEN-GL04C geoid was used to convert ellipsoidal heights to geoidal values [Forste *et al.*, 2008]. This geoid was calculated from GRACE satellite data supplemented by surface gravity data from altimetry and gravimetry.

[13] The firm density correction is required to account for the fact that solid ice occurs at depth and above this is a layer of firm (compacted snow) with a density less than that of solid ice. There are few measurements of this parameter as it can only be determined in situ so modelled parameters are used throughout this study. A regional atmosphere model [Van de Berg *et al.*, 2005, 2006] was run on a 55 km grid and the output of the model used in a steady-state firm densification model which takes account of temperature, accumulation and wind speed variability [Helsen *et al.*, 2008]. The model compares well with ice core density profiles with the exception of one core where horizontal compression, which is not represented in the model, is believed to be important [van den Broeke, 2008]. An advantage of this method is that spatial variability, which is modelled to have a standard deviation of around 24%, is captured which is generally missed by in situ measurements or regression against measured ice thickness [e.g., Bamber and Bentley, 1994]. For Larsen C it is expected that the model will overestimate the firm density corrections as it takes no account of surface melting. To account for this, the firm density correction was reduced to have a mean of 10 m, based on in situ measurements in West Antarctica (H. Corr,

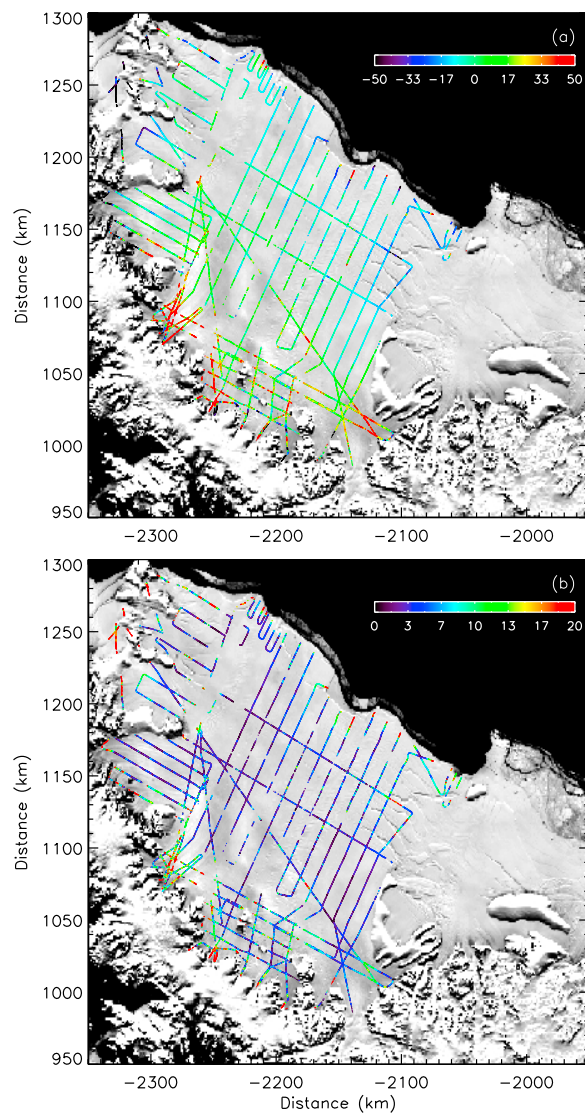


**Figure 2.** (a) Difference between ERS-derived thickness and thickness measurements from BAS/Argentine airborne measurements overlaid on MOA image of the region. (b) As Figure 2a but for percentage differences.

British Antarctic Survey, personal communication, 2009), but maintaining the spatial pattern as shown in the inset of Figure 1a.  $1027 \text{ kg m}^{-3}$  and  $917 \text{ kg m}^{-3}$  were used as the density of water and ice respectively. Small areas where the firm density correction is larger than surface elevation, causing negative thicknesses, in the south are set to zero. This is in an area of rifting where the mean density of the ice column is indeterminate. The resulting ice thickness estimates are shown as the coloured background in Figure 1a.

#### 4. Results and Validation

[14] To determine the quality of the ERS-1 RA data, the elevations were compared against release 428 ICESat data [Zwally *et al.*, 2007]. These data were recorded between 2003 and 2008 with the laser being switched on 2–3 times a year, evenly spaced through the year. The accuracy of the ICESat data have been shown to be on the order of 20 cm

for low slopes [Brenner *et al.*, 2007]. The same tide model was used for the ICESat data as for ERS-1 RA.

[15] The differences are shown in Figure 1b and have a mean of  $-2.3 \text{ m}$  (ICESat-elevation grid) with a root mean squared (RMS) difference of  $4.9 \text{ m}$  and standard deviation of  $4.35 \text{ m}$ . The differences have a gradient towards negative values at the northerly end of the ice shelf. The gradient and the magnitude of the differences agrees with the thinning rate shown by Zwally *et al.* [2005] and Shepherd *et al.* [2003], who described thinning across the ice shelf with small annual rates at the southern end rising to  $\sim 30 \text{ cm a}^{-1}$  at the northern end. The mean difference reduced to  $-1.7 \pm 4.5 \text{ m}$  when a temporal correction from  $\text{dH/dt}$  measurements calculated by Zwally *et al.* [2005] was applied to the elevations. The spread on the measurement is small with a large part contributed by the region at the southern most end of the ice shelf where large rifts in the ice shelf are seen in visible imagery. When only the central area is considered (see red box on Figure 1a) along with the temporal correction, a mean bias of  $-0.5 \pm 1.1 \text{ m}$  is obtained. The size of this variability is lower than that seen in a validation of a whole Antarctica DEM [Bamber *et al.*, 2009; Griggs and Bamber, 2009] justifying the tailored approach for the ice shelves used here.

[16] For the validation of the thickness retrieval, data from a British Antarctic Survey/Argentine survey of the ice shelf in 1997–8 were used [Holland *et al.*, 2009]. The survey used differential GPS and radar transmitting at about  $150 \text{ MHz}$ . Crossover analysis of the results showed an RMS difference of  $12 \text{ m}$  with horizontal positioning accurate to less than  $0.5 \text{ m}$  [Holland *et al.*, 2009]. Flights were flown in a near grid with even coverage over most of Larsen C, excluding the heavily rifted zone to the south and are corrected for the spatial variations in firm density [Helsen *et al.*, 2008] with reduced mean to account for melting. We used this dataset as it is the most complete in terms of spatial sampling and is temporally close to the 1995 time stamp of the thickness estimates. Figure 2 shows the spatial distribution of differences between the airborne data and ERS-1 RA-based thicknesses (airborne thickness-ERS thickness). A gradient in error over the ice shelf with negative errors indicating that the satellite thickness grid is too thick in the southern portion and too thin in the northern portion is evident. This gradient is in the opposite sense to that which would be expected from known thinning although with only three years between the two datasets, significant thinning is not expected. The gradient is in the same sense as the gradient in firm correction from the modelled estimate indicating that a better representation of melting in the firm model may explain the differences.

[17] Figure 3 shows a histogram of the differences between the airborne and satellite estimates of ice thickness for the whole ice shelf. The mean bias is  $-0.22 \text{ m}$  with a standard deviation and RMS difference of  $36.7 \text{ m}$ . Using the modelled firm correction without reducing its mean to account for melting increases the bias to  $+23.2 \text{ m}$  with a standard deviation of  $43.67 \text{ m}$  and RMS difference of  $37.03 \text{ m}$  showing the large effect of correctly determining the firm depth. In the central area where estimates are expected to be most accurate, the mean difference is  $-2.03 \text{ m}$  with a standard deviation of  $11.04 \text{ m}$  and RMS difference of  $10.85 \text{ m}$ . The random error in the differences is



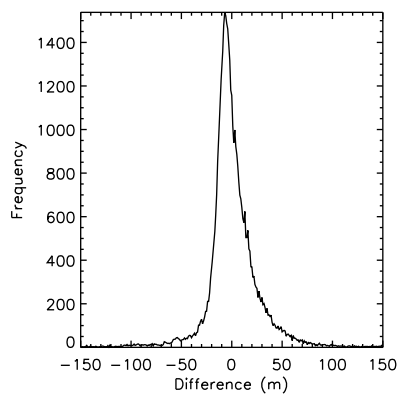


**Figure 3.** Histogram of the differences between ERS-derived thickness grid and thickness measurements from BAS/Argentine airborne measurements.

less than the 12 m error in the airborne data. A bias of  $-2.03$  m is only representative of an error in elevation of less than half a metre which is much lower than the error in the most recent DEM of Antarctica over the ice shelves [Griggs and Bamber, 2009] and Larsen C gives a “worst case” scenario for expected errors in ice shelf thickness retrievals due to its location and surface melting. Within 10 km of the grounding line, the mean bias is  $-1.45$  m with a standard deviation and RMS of 68.5 m, about six times the random error in the central region although the ice is significantly thicker so percentage errors are similar. There is little validation data in the areas of rifting seen at the southern- and northern-most ends of the ice shelf but estimates are not expected to be accurate there as the density of the shelf, over a radar footprint, will be lower than elsewhere and indeterminate.

#### 4.1. Error Analysis

[18] All the parameters in equation (1) induce error in estimates of ice thickness and it is possible that they may cancel each other out, implying a smaller error in comparison with airborne data than the true maximum error. We discuss each parameter in turn.

#### 4.2. Surface Elevation

[19] The surface elevations have been compared to independent estimates for the ice shelf. A bias and standard deviation of  $-1.7$  m and 4.5 m respectively is found when accounting for the time difference between the two measurements. This analysis was performed on the elevation with respect to the WGS 84 ellipsoid and so error in the geoid adds further error to our estimates of ice thickness. Analysis of the EIGEN-GL04C geoid gives a total error of 0.23 m and an RMS difference of up to 0.36 m when compared to independent GPS derived geoid heights [Forste et al., 2008]. Thus, the total error in the surface elevation measurements is 4.51 m.

#### 4.3. Ice Density

[20] Throughout the calculations, we used a mean ice density of  $917 \text{ kg m}^{-3}$ , the density of pure ice. Fricker et al. [2001] used a model of ice density constrained by temperature measurements from boreholes and found values between 912 and  $922 \text{ kg m}^{-3}$  for column averaged ice density on the Amery Ice Shelf. This suggests an error of  $\pm 5 \text{ kg m}^{-3}$  for meteoric ice density.

[21] Although an analysis of ice thickness data suggests that marine ice extends in bands from the grounding line to the ice front [Holland et al., 2009], it is presumed to have a density close to  $917 \text{ kg m}^{-3}$  as used for the Amery by Fricker et al. [2001] implying no additional error due to the presence of marine ice.

#### 4.4. Water Density

[22] A value of  $1027 \text{ kg m}^{-3}$  is used for water density which is the mean global sea water density. Bamber and Bentley [1994] report a value of  $1024 \text{ kg m}^{-3}$  for the Ross Ice Shelf, and Fricker et al. [2001] use a value of  $1029 \text{ kg m}^{-3}$  from an ocean measurement near the Amery. We estimate that the error in water density is  $\pm 3 \text{ kg m}^{-3}$ .

#### 4.5. Firn Density Correction

[23] As discussed in the methodology, firn density correction is difficult to estimate, particularly for ice shelves with melting surfaces which models do not represent. In situ values of the firn density correction have been measured at 10 m (H. Corr, British Antarctic Survey, personal communication, 2009) and 9 m [Renner, 1969]. An airborne traverse of Larsen C measuring ice thickness and surface elevation was undertaken in 2004 [Rignot et al., 2004b]. From these data, a mean firn density correction (i.e., with no spatial variation) can be inferred by solving equation (1). This produced a mean firn density correction of 8.63 m. Thus, we estimate the error on this correction to be about  $\pm 1.5$  m.

[24] Combining these errors in quadrature gives a mean random error on the ice shelf of 47.3 m, which is about 10 m higher than the validation suggests indicating that some of the errors may be cancelling each other. Errors close to the grounding zone are larger than those nearer the ice front but due to the thicker ice in this region, percentage errors are smaller. The airborne dataset of ice thickness has an RMS difference of 12 m ignoring error in firn correction which is considered constant. Therefore, considering the complete spatial coverage provided by the satellite retrieval method, we find that ice thickness can be retrieved from satellite altimetry with acceptable errors for modelling and mass budget calculations. The ice thickness close to the grounding lines of the larger ice shelves is typically in the range 600–1500 m [Rignot et al., 2008]. Assuming similar errors to those obtained here, near the grounding line, suggests an error in thickness for the larger shelves of 5–10%. However, as Larsen C is our “worst case” ice shelf, we expect errors in the retrieval of ice thickness from satellite altimetry to be significantly lower on other ice shelves where surface elevation and firn density correction can both be estimated with greater accuracy.

### 5. Conclusions

[25] Ice thickness estimates for Larsen C were inferred from estimates of surface elevation from the ERS-1 radar altimeter and firn density correction estimated using the output of a regional climate model. Surface elevations were determined with a bias of  $-1.7$  m and random error of 4.5 m when corrected for temporal differences between the two data sets used. Comparison of the calculated ice thickness with independent airborne estimates of ice thickness shows a bias of  $-0.22$  m and a random error of 36.7 m. Calculations

lations of maximum error suggest a value of around 47 m. Overall, we show that ice thickness can be determined to high accuracy at high spatial resolution from the geodetic phase of ERS-1.

[26] **Acknowledgments.** The authors would like to thank the following data contributors: CReSIS, University of Kansas, for the in situ ice thickness profile, H. Corr (British Antarctic Survey) for the in situ ice thickness validation data, W. Krabill (NASA Goddard Wallops Flight Facility) for the surface elevation profile, H. J. Zwally (NASA Goddard Space Flight Center) for the elevation change data, and M. van den Broeke (IMAU, Utrecht University) for the firm correction. This work was supported by NERC grant NE/E004032/1.

## References

- Bamber, J., and C. R. Bentley (1994), A comparison of satellite-altimetry and ice-thickness measurements of the Ross Ice Shelf, Antarctica, *Ann. Glaciol.*, **20**, 357–364.
- Bamber, J. L., and R. A. Bindshadler (1997), An improved elevation dataset for climate and ice-sheet modelling: Validation with satellite imagery, *Ann. Glaciol.*, **25**, 439–444.
- Bamber, J., and J. L. Gomez-Dans (2005), The accuracy of digital elevation models of the Antarctic continent, *Earth Planet. Sci. Lett.*, **237**, 516–523, doi:10.1016/j.epsl.2005.06.008.
- Bamber, J. L., et al. (2009), A new 1 km digital elevation model of Antarctica derived from combined radar and laser data, Part I: Data and methods, *Cryosphere*, **3**, 101–111.
- Brenner, A. C., et al. (2007), Precision and accuracy of satellite radar and laser altimeter data over the continental ice sheets, *IEEE Trans. Geosci. Remote Sens.*, **45**, 321–331, doi:10.1109/TGRS.2006.887172.
- De Angelis, H., and P. Skvarca (2003), Glacier surge after ice shelf collapse, *Science*, **299**, 1560–1562, doi:10.1126/science.1077987.
- Deutsch, C. L., and A. G. Journel (1997), *GSLIB: Geostatistical Software Library and User's Guide*, 2nd ed., 369 pp., Oxford Univ. Press, Oxford, U. K.
- Egbert, G. D., and S. Y. Erofeeva (2002), Efficient inverse modeling of barotropic ocean tides, *J. Atmos. Oceanic Technol.*, **19**, 183–204, doi:10.1175/1520-0426(2002)019<0183:EIMOB>2.0.CO;2.
- Forste, C., et al. (2008), The GeoForschungsZentrum Potsdam/Groupe de Recherche de Geodesie Spatiale satellite-only and combined gravity field models: EIGEN-GL04S1 and EIGEN-GL04C, *J. Geod.*, **82**, 331–346, doi:10.1007/s00190-007-0183-8.
- Fricker, H. A., and L. Padman (2006), Ice shelf grounding zone structure from ICESat laser altimetry, *Geophys. Res. Lett.*, **33**, L15502, doi:10.1029/2006GL026907.
- Fricker, H. A., S. Popov, I. Allison, and N. Young (2001), Distribution of marine ice beneath the Amery Ice Shelf, *Geophys. Res. Lett.*, **28**, 2241–2244, doi:10.1029/2000GL012461.
- Griggs, J. A., and J. L. Bamber (2009), A new 1 km digital elevation model of Antarctica derived from combined radar and laser data. Part II: Validation and error estimates, *Cryosphere*, **3**, 113–123.
- Haran, T. R., et al. (2005, updated 2006), MODIS Mosaic of Antarctic (MOA) Image Map, <http://nsidc.org/data/nsidc-0280.html>, Natl. Snow and Ice Data Cent., Boulder, Colo.
- Helsen, M. M., et al. (2008), Elevation changes in Antarctica mainly determined by accumulation variability, *Science*, **320**, 1626–1629, doi:10.1126/science.1153894.
- Holland, P. R., H. F. J. Corr, D. G. Vaughan, A. Jenkins, and P. Skvarca (2009), Marine ice in Larsen Ice Shelf, *Geophys. Res. Lett.*, **36**, L11604, doi:10.1029/2009GL038162.
- King, M. A., and L. Padman (2005), Accuracy assessment of ocean tide models around Antarctica, *Geophys. Res. Lett.*, **32**, L23608, doi:10.1029/2005GL023901.
- Renner, R. G. B. (1969), Surface elevations on the Larsen Ice Shelf, *Br. Antarct. Surv. Bull.*, **19**, 1–8.
- Rignot, E. (1996), Tidal motion, ice velocity and melt rate of Petermann Gletscher, Greenland, measured from radar interferometry, *J. Glaciol.*, **42**, 476–485.
- Rignot, E. (2001), Evidence for rapid retreat and mass loss of Thwaites Glacier, West Antarctica, *J. Glaciol.*, **47**, 213–222, doi:10.3189/172756501781832340.
- Rignot, E., and R. H. Thomas (2002), Mass balance of polar ice sheets, *Science*, **297**, 1502–1506, doi:10.1126/science.1073888.
- Rignot, E., G. Casassa, P. Gogineni, W. Krabill, A. Rivera, and R. Thomas (2004a), Accelerated ice discharge from the Antarctic Peninsula following the collapse of Larsen B ice shelf, *Geophys. Res. Lett.*, **31**, L18401, doi:10.1029/2004GL020697.
- Rignot, E., et al. (2004b), Improved estimation of the mass balance of glaciers draining into the Amundsen Sea sector of West Antarctica from the CECS/NASA 2002 campaign, *Ann. Glaciol.*, **39**, 231–237, doi:10.3189/172756404781813916.
- Rignot, E., et al. (2008), Recent Antarctic ice mass loss from radar interferometry and regional climate modelling, *Nat. Geosci.*, **1**, 106–110, doi:10.1038/ngeo102.
- Rott, H., et al. (1996), Rapid collapse of northern Larsen Ice Shelf, *Antarct. Sci.*, **271**, 788–792.
- Scambos, T. A., J. A. Bohlander, C. A. Shuman, and P. Skvarca (2004), Glacier acceleration and thinning after ice shelf collapse in the Larsen B embayment, Antarctica, *Geophys. Res. Lett.*, **31**, L18402, doi:10.1029/2004GL020670.
- Scambos, T. A., et al. (2007), MODIS-based Mosaic of Antarctica (MOA) data sets: Continent-wide surface morphology and snow grain size, *Remote Sens. Environ.*, **111**, 242–257, doi:10.1016/j.rse.2006.12.020.
- Shepherd, A., et al. (2003), Larsen ice shelf has progressively thinned, *Science*, **302**, 856–859, doi:10.1126/science.1089768.
- Van de Berg, W. J., et al. (2005), Characteristics of the Antarctic surface mass balance, 1958–2002, using a regional atmosphere climate model, *Ann. Glaciol.*, **41**, 97–104, doi:10.3189/172756405781813302.
- Van de Berg, W. J., M. R. van den Broeke, C. H. Reijmer, and E. van Meijgaard (2006), Reassessment of the Antarctic surface mass balance using calibrated output of a regional atmospheric climate model, *J. Geophys. Res.*, **111**, D11104, doi:10.1029/2005JD006495.
- van den Broeke, M. (2008), Depth and density of the Antarctic firm layer, *Arct. Antarct. Alp. Res.*, **40**, 432–438, doi:10.1657/1523-0430(07-021)[BROEKE]2.0.CO;2.
- Zwally, H. J., et al. (2005), Mass changes of the Greenland and Antarctic ice sheets and shelves and contributions to sea-level rise: 1992–2002, *J. Glaciol.*, **51**, 509–527, doi:10.3189/172756505781829007.
- Zwally, H. J., et al. (2007), GLAS/ICESat L2 Antarctic and Greenland Ice Sheet Altimetry Data V428: 25 September 2003 to 27 November 2006, <http://nsidc.org/data/gla12.html>, Natl. Snow and Ice Data Cent., Boulder, Colo.

J. L. Bamber and J. A. Griggs, Bristol Glaciology Centre, School of Geographical Sciences, University of Bristol, Bristol BS8 1SS, UK.